A CONSIDERATION OF EXPERIMENTAL UNCERTAINTIES FOR PREDICTING CHF IN ROD BUNDLES

Dae-Hyun Hwang, Seong-Jin Kim, Hyuk Kwon, and Kyong-Won Seo
Korea Atomic Energy Research Institute
989-111 Daedeok-daero, Yuseong, Daejeon, 305-353, Korea
dhhwang@kaeri.re.kr; sjkim2@kaeri.re.kr; kwonhk@kaeri.re.kr; nulmiso@kaeri.re.kr

ABSTRACT

The influence of CHF experimental uncertainties on predicting the CHF in rod bundles was examined with a local parameter CHF prediction model. The AECL-IPPE 1995 CHF lookup table method, in conjunction with a subchannel analysis code MATRA, was employed with various correction factors. Referring to the verification and validation procedure issued by ASME, the validation uncertainty for a selected CHF data from the rod bundle CHF experiment was evaluated by the sensitivity coefficient approach and the Monte-Carlo approach. Thirteen uncertainty parameters were selected for the sensitivity and uncertainty analyses: five state parameters, two geometry parameters, and six modeling parameters. The validation uncertainty with respect to the DNBR (i.e., predicted-to-measured CHF ratio) was estimated by accounting for the measurement uncertainty, input uncertainty, and numerical uncertainty. Finally, the influence of experimental uncertainties to the correlation limit DNBR was illustrated by incorporating the validation uncertainty into the selected CHF database.

KEYWORDS
Experimental uncertainty, Limit DNBR, ASME V&V 20, CHF lookup table, SMART

1. INTRODUCTION

The critical heat flux (CHF) is an important parameter in the design of an advanced water cooled nuclear reactor to avoid fuel failure caused by a deterioration of the heat transfer coefficient in the core. The design criteria specifies that the nuclear reactor must be operated at a certain percentage below the CHF at all times and locations. This is accomplished by comparing the minimum DNBR (Departure from Nucleate Boiling Ratio) in the reactor core with a limit DNBR, which was determined by considering the uncertainty of the CHF prediction model. According to the CHF design criterion, the CHF should not occur at the hottest rod in the core during normal operation and anticipated operational occurrences with at least a 95% probability at a 95% confidence level. To incorporate this design criterion into the correlation limit DNBR, it is necessary to evaluate the tolerance limit of M/P (Measured CHF divided by Predicted CHF) from the sample distribution of M/P, which is drawn from an analysis of the CHF data. The sample distribution of M/P represents the uncertainty of the CHF prediction model. The inverse of the lower tolerance limit of M/P corresponds to the limit DNBR.

In the open-latticed fuel assemblies such as in PWR cores, the CHF is usually calculated by the local parameter CHF correlation. It requires local thermal hydraulic parameters at the CHF location which are usually calculated by a subchannel analysis code. In a conventional approach, the M/P for the CHF data is evaluated by comparing the nominal values of the predicted and measured CHFs. That is, the experimental uncertainty for the CHF data was not clearly accounted for in the procedure to determine the limit DNBR. However, since the local thermal hydraulic parameters are not measured during CHF experiments, the measurement uncertainties of the bundle averaged parameters propagate to the

uncertainties of the local parameters through a subchannel analysis code. Thus, the uncertainties of local parameters as well as the uncertainty of measured CHF should be considered to evaluate the uncertainty of the CHF prediction model.

In this study, the influence of experimental uncertainty to the uncertainty of the CHF prediction model was investigated. Rod bundle CHF data obtained under an advanced PWR core condition were applied to evaluate the uncertainty of a CHF prediction model. The AECL-IPPE 1995 CHF lookup table method [1] was selected as the local parameter CHF correlation, with appropriate correction factors developed for rod bundles. Referring to the verification and validation (V&V) procedure for a heat transfer model described in the ASME V&V-20 [2], the validation uncertainty of the CHF table method was estimated against a rod bundle CHF data by employing a subchannel analysis code, MATRA.

2. ASSESSMENT OF CHF LOOKUP TABLE EMTHOD FOR ROD BUNDLES

2.1. CHF Experiments under Advanced PWR Conditions

The CHF experiment has been conducted in a high-pressure water test loop at Stern Laboratories in Canada. The test bundle simulates fuel assembly which is applicable to an advanced PWR developed at KAERI, called SMART (System-integrated Modular Advanced ReacTor) [3]. As illustrated in Fig. 1, the major components of the test loop consists of test section, gas pressurizer, mixers, heat exchangers, condenser, main coolant pump, and preheater. The test section includes the pressure housing, flow channel, fuel simulators, spacer grids, and instrumentation. Four different test bundles were employed to investigate the influence of non-uniform axial power shape and a central unheated rod on the CHF. The test bundle consists of twenty-five indirectly heated rods with a 9.5 mm outer diameter. The test section and test loop were instrumented to measure the power, flow rate, absolute/differential pressures, and coolant temperature during testing. The uncertainties of the heater rods/flow channel dimensions and the test conditions were originated from the fabrication tolerance and instrumentation errors. The uncertainty of the measured critical heat flux was estimated as $\pm 0.68\%$.

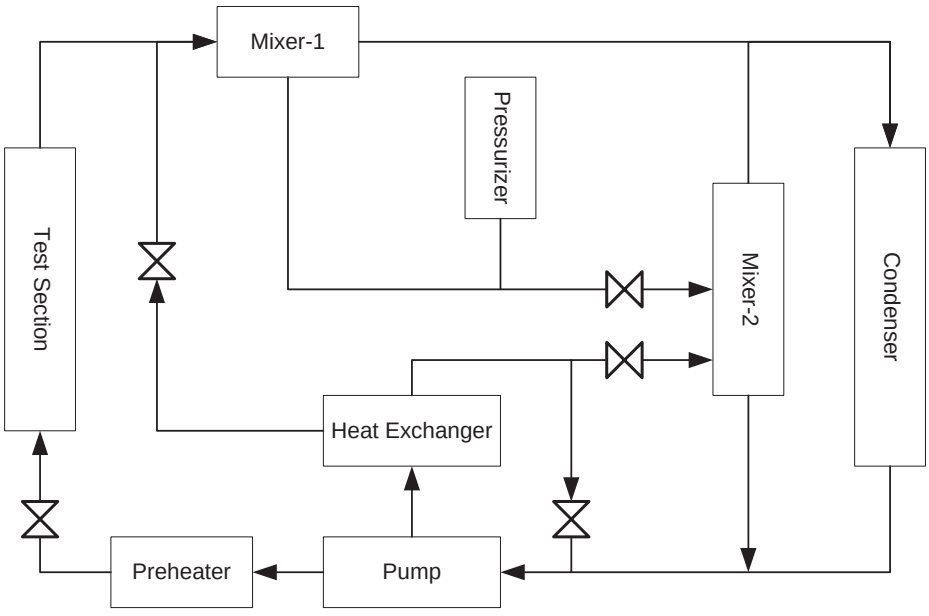

Figure 1. Schematic of CHF Test Loop.

Adiabatic pressure drop tests were performed at the beginning of each test series to check the reproducibility of the data. Single-phase and two-phase pressure drops in the test bundle were measured during the CHF experiments. A thermal mixing test was separately performed by measuring the subchannel exit temperatures under steady-state conditions. A large gradient of radial power distribution was applied for the thermal mixing test bundle: the average power in the hot region is approximately 4.5 times higher than that in the cold region. A CHF test has been conducted in a pressure range of 25 to 17 MPa, a mass flux of 500 to 2500 kg/m^{2}s, an inlet temperature of 150 to 325 deg-C, and a critical quality of -25% to +74%. The effects of a non-uniform axial power shape and unheated rod were investigated during the CHF experiments.

2.2. Application of a CHF Lookup Table Method to Rod Bundles

The CHF lookup table method provides CHF values for water-cooled tubes at discrete values of pressure, mass velocity, and critical quality. Linear interpolation between table values gives the CHF for a specific condition, and several correction factors were introduced to extent the CHF table to various shapes of the boiling channel. It has been reported that the CHF lookup table method revealed a reasonable accuracy for rod bundles with appropriate correction factors [4-6]. In this study, the AECL-IPPE 1995 CHF lookup table was selected as the local parameter CHF prediction model. The local thermal hydraulic conditions were calculated by the subchannel analysis code, MATRA. The CHF was determined at the predicted minimum DNBR location with a heat balance method (HBM) [7]. In addition to the existing correction factors for rod bundles (K_1, K_3, and K_4) [1], a complementary correction factor for rod bundles (K_R) was developed from an extensive assessment of rod bundle CHF data for PWR and advanced PWR conditions. The functional form of the correction factors are provided in Table I. Tong's F-factor [8] was applied for axially non-uniform power shapes. Based on the local mass flux, local quality, and pressure calculated by the MATRA code, the CHF for uniform axial power shape is calculated by

$$q''_{CHF} = q''_{D=8} \times K_1 \times K_3 \times K_4 \times K_5 \times K_R \tag{1}$$

Table I. Correction factors of a CHF Table Method for Rod Bundles

Description	Correction factors
Channel flow area	$K_1 = \left(8/d_{hy}\right)^{0.5}$, for $2 < d_{hy} < 25$; $K_1 = 2$, for $d_{hy} < 2$; $K_1 = 0.566$, for $d_{hy} > 25$
Spacer grid	$K_3 = 1 + 1.5 \times \sqrt{K_{grid}} \times \left(G \times 10^{-3}\right)^{0.2} \times \exp\left[-0.1 \times g_{sp}/d_{hy}\right]$
Heated length	$K_4 = \exp\left[e^{2\alpha} \times d_{he}/z\right]$, for $z \geq 5 \times d_{he}$; $K_4 = 1$, otherwise
Non-uniform APS	$K_5 = q''_{loc} \left\{1 - e^{-C(z_C - z_{ONB})}\right\} \Big/ C \int_{z_{ONB}}^{z_C} q'' e^{-C(z_C - z)} dz$, $C = 5.906 \times \frac{\left(1 - \chi_C\right)^{4.31}}{\left(G/1356\right)^{0.478}}$ (m^{-1})
Rod bundles	$K_R = \left\{1.062 - 0.47 \times \exp\left(-4.4 \times P_r\right)\right\} \times \left\{1.029 - 5.14\text{E-}5 \times g_{sp}\right\} \times \left\{0.966 + 1.27\text{E-}5 \times G\right\}$

The accuracy of the CHF table method with modified correction factors was examined for the CHF data obtained from four different SMART test bundles. The mean and standard deviation of M/P were calculated by 1.011 and 0.090, respectively. The distribution of M/P was compared with the normal distribution curve in Fig. 2. As a result of a Kolmogorov-Smirnov normality test, the data were drawn from a normally distributed population at the 5% significance level. Thus, according to a traditional approach, the limit DNBR of the CHF table method can be evaluated by

$$DNBR_{Limit} = \frac{1}{(M/P)_{mean} - k_{95/95} \cdot s} \tag{2}$$

where '$(M/P)_{\text{mean}}$' is the mean value of M/P, 's' is the sample standard deviation of M/P, and $k_{95/95}$ is the one-sided tolerance limit factor [9], which was determined as 1.772 for 437 data points. As a result, the limit DNBR was evaluated as 1.174.

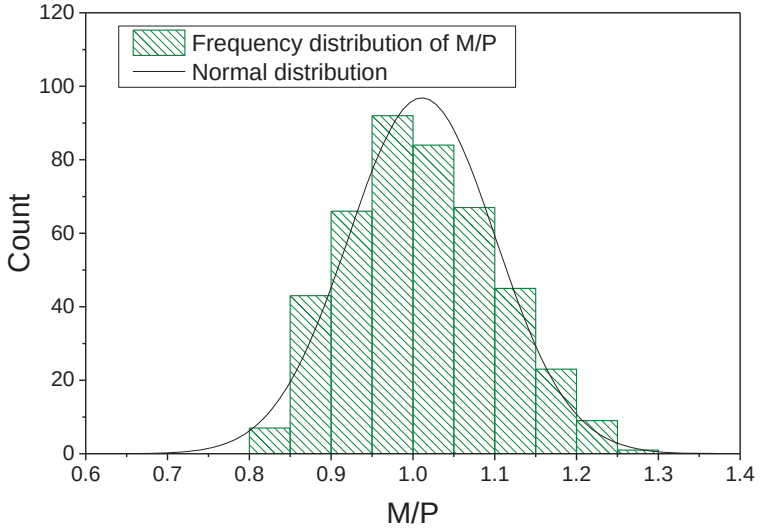

Figure 2. Distribution of M/P by a CHF table method

3. UNCERTAINTY ANALYSIS OF CHF PREDICTION MODEL

3.1. Methodology for Uncertainty Analysis

The uncertainty of the CHF prediction model was estimated against selected steady-state CHF data according to the standard of the V&V procedure issued by ASME [2]. The final goal of this standard is to evaluate the uncertainty range of the model error from the validation comparison error and the validation uncertainty. The validation comparison error (E) is defined as the difference between the simulation result (P) and measured data (M). From the definition of an error, E can be expressed as a difference between the simulation error (δ_P) and the measure data error (δ_M). Thus E contains all of the errors relevant to the simulation procedure and the experimental results. The simulation error accounts for various errors: a model error (δ_{model}) due to modeling assumptions and approximations, a numerical error (δ_{num}) due to the numerical solution method of the equations, and an input error (δ_{input}) due to errors in the simulation input parameters. Thus, the error of the CHF prediction model, δ_{model}, can be expressed as

$$\delta_{\text{model}} = E - \left(\delta_{num} + \delta_{input} - \delta_M \right) \tag{3}$$

The uncertainty range of the model error can be estimated from E and the validation uncertainty (u_{val}) which is defined as an estimate of the standard deviation of the combined errors in the parenthesis of eq. (3). If these errors are statistically independent, the validation uncertainty can be estimated by

$$u_{val} = \sqrt{u_{num}^2 + u_{input}^2 + u_M^2} \tag{4}$$

where the standard uncertainties u_{num}, u_{input}, and u_M are the estimates of errors δ_{num}, δ_{input}, and δ_M, respectively. From eq. (3), the uncertainty range of the model error can be estimated as

$$E - u_{val} \le \delta_{model} \le E + u_{val} \tag{5}$$

In eq. (4), the numerical uncertainty (u_{num}) can be estimated from the code/solution verification while the measurement uncertainty (u_M) is determined from the instrument error during the experiment. For the estimation of input uncertainty (u_{input}), two approaches were applied for an analysis of the uncertainty propagation of input parameters to the simulation results: a sensitivity coefficient (SC) approach and a Monte-Carlo (MC) approach. In the SC approach, as shown in Fig. 3, the local sensitivity coefficient is calculated under nominal conditions. The input uncertainty is calculated by combining the sensitivity coefficients and the coefficient of variations for each input parameter. That is,

$$u_{input} = \sqrt{\sum_k^{all} \left(S_k \frac{\sigma_k}{\mu_k} \right)^2} \tag{6}$$

In this study the simulation results are expressed as DNBR, which represents the ratio of predicted-to-measured CHF. Then a new validation comparison error was introduced which is expressed by the normalized P/M: i.e., $E = \mu_{P/M} - 1$, where $\mu_{P/M} = (P/M)/(P/M)_0$.

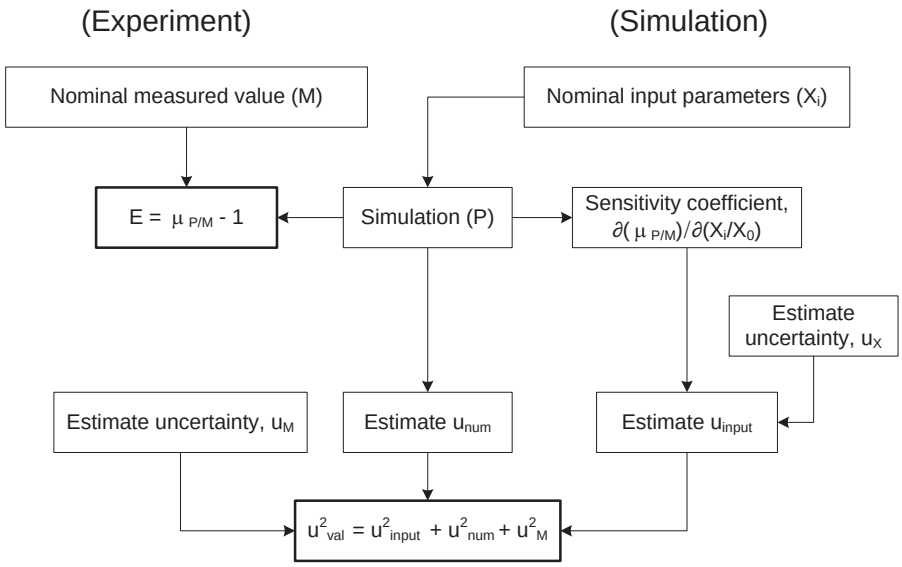

Figure 3. Uncertainty analysis by sensitivity coefficient approach

In the MC approach, as shown in Fig. 4, the input uncertainty can be estimated by a simple random sampling for each input parameter. For a set of random sampled input parameters, the simulation result (P_i) is compared with the random sampled experimental data (M_i). After a number of samples, a distribution of E can be obtained which included the input measurement uncertainties.

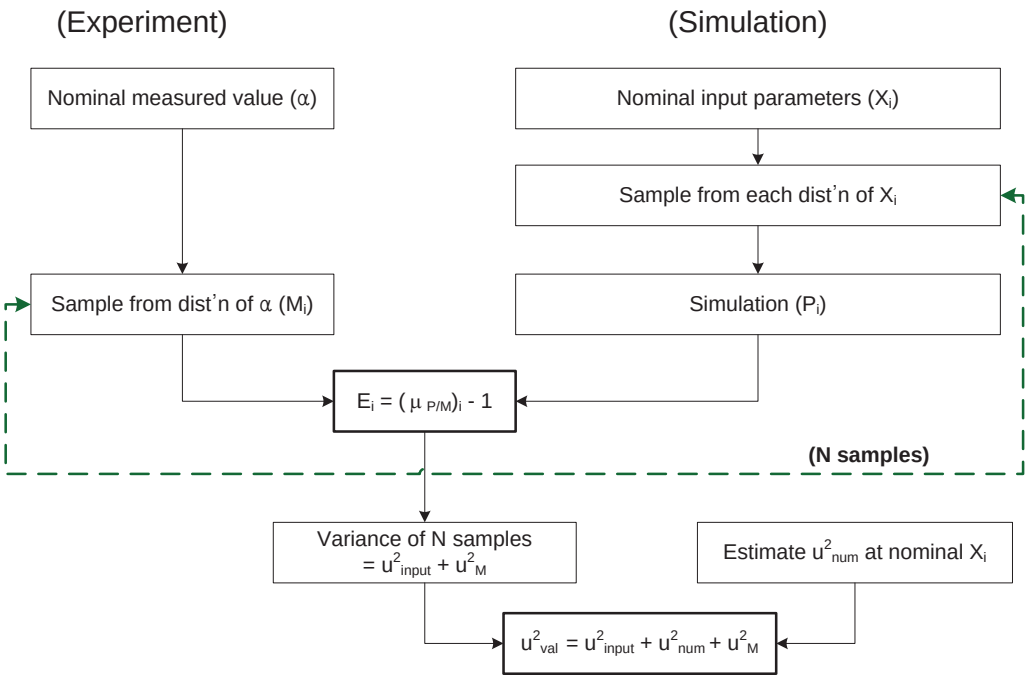

Figure 4. Uncertainty analysis by Monte-Carlo approach

3.2. Uncertainty Parameters

A steady-state rod bundle CHF data for a SMART test bundle with non-uniform axial power shape was selected for an uncertainty analysis of the CHF prediction model. The uncertainty parameters for the evaluation of input uncertainty were selected by considering the uncertainties of experimental parameters and the MATRA code models. The estimated values of the standard deviation and probability distribution function (pdf) for each parameter are listed in Table II. The probability distribution functions for all parameters were assumed as normal except the inlet temperature which has a flat distribution.

The uncertainties of the test condition and test section geometry were determined from the instrumentation and fabrication errors for the CHF experiment. The power distribution uncertainty was accounted for in the Monte-Carlo approach by re-normalizing the power distribution after a random sampling of power at every calculation node. The uncertainty parameters for the MATRA code model were selected which may have significant influence on the distribution of local thermal hydraulic conditions in the subchannels. The uncertainties of the model parameters were evaluated on the basis of relevant experimental data for rod bundles, if available.

The uncertainty of the single-phase bundle friction factor by the McAdams relation was assumed to be 10%. The optimum value of the grid loss factor was determined from an analysis of the single-phase pressure drop data for the whole length of the SMART test bundles, which included pressure losses due to the bundle friction and spacer grids. The uncertainty of grid loss factor accompanied with the McAdams friction factor model was evaluated as 1.8%.

The two-phase pressure drop was measured over the test bundles during the CHF experiments. A set of two-phase models was selected for the evaluation of the two-phase pressure drop data: a Saha-Zuber subcooled void model, Chexal-Lellouch bulk void model, and homogeneous two-phase friction multiplier model. As a result of the evaluation, it was revealed that the MATRA code with this set of two-phase models under-predict the two-phase pressure drop over the test bundles by about 12%. The uncertainty

estimated by this set of models was imposed on the uncertainty of two-phase friction multiplier model. On the other hand, the uncertainties of other models were assumed by referring to a previous work for PSBT benchmark exercises [10].

Turbulent mixing parameter (β) is an important input variable of the MATRA code, which is defined as a ratio of the lateral fluctuating mass flux to the axial mass flux of the fluid in the subchannel. The optimum value of β was determined from the analysis of the thermal mixing test data, which provided subchannel exit temperatures for a test bundle with a large gradient of radial power distribution. As a result of the analysis for 106 test data from a SMART test bundle, the mean value and standard deviation of β were evaluated as 0.062 and 0.005, respectively.

The uncertainty distributions evaluated from the relevant experimental data for the SMART test bundles are illustrated in Fig. 5: the grid loss factor, two-phase friction multiplier model, and turbulent mixing parameter.

Table II. Uncertainty parameters

Parameter	Nominal	1-σ	pdf
Test conditions:			
Pressure, MPa	15.57	0.048	Normal
Inlet temperature, ^{o}C	280.2	0.4	Flat
Inlet mass flux, kg/m^{2}s	1002	9.5	Normal
Average heat flux, kW/m^2	1058	7.2	Normal
Power distribution	Non-uniform	1.7%	Normal
Geometry:, mm			
Rod diameter	9.5	0.03	Normal
TS channel width	65.61	0.03	Normal
Modeling:			
Bundle friction factor	$0.184Re^{-0.2}$	10%	Normal
Grid loss factor	1.0	1.8%	Normal
Turbulent mixing parameter	0.062	0.005	Normal
Subcooled void model	1.0	10%	Normal
Bulk void model	1.0	10%	Normal
Two-phase friction multiplier	0.881	10.3%	Normal

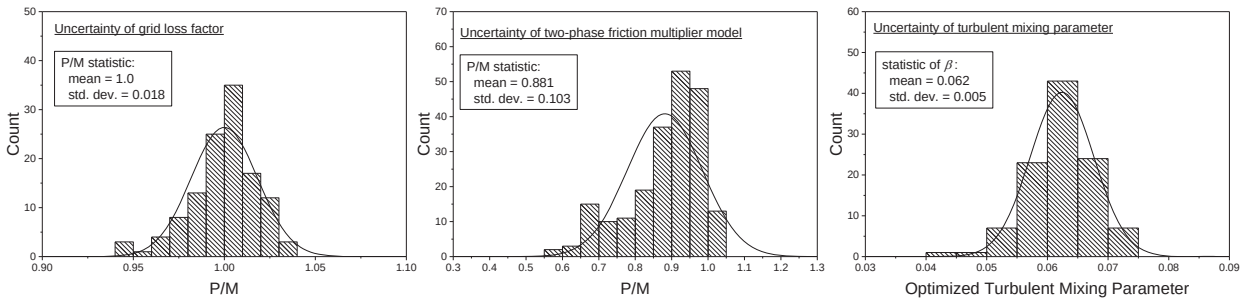

Figure 5. Uncertainty distributions of the MATRA code models

3.3. Sensitivity Coefficient Approach

The sensitivity coefficient (S_i) is defined as the ratio between the percent change of DNBR to the percent change of input parameter. It is evaluated by changing the parameter in $\pm 3\sigma$ from its nominal value. The sensitivity coefficients for uncertainty parameters are compared in Fig. 6. The coefficient for each uncertainty parameter was calculated by the AECL-IPPE 1995 CHF table with HBM at the nominal condition. As a result of the analysis, the maximum sensitivity appeared for the inlet temperature variation. Actually, the importance of a parameter to the overall uncertainty is not in accordance with the magnitude of sensitivity coefficient. The contribution of a parameter to the overall uncertainty can be estimated from the importance factor (*IF*), which is calculated by combining the coefficient of variation and the sensitivity coefficient. For a parameter *i*, it is calculated by

$$IF_i = \frac{\left[S_i\left(\sigma_i/\mu_i\right)\right]^2}{\sum_{k}^{all}\left[S_k\left(\sigma_k/\mu_k\right)\right]^2} \tag{7}$$

According to the importance factor, major contributions to the overall uncertainty of DNBR were due to the heat flux, inlet mass flux, turbulent mixing parameter, inlet temperature, and bulk void model. For the selected CHF data provided in Table II, the input uncertainty was estimated as 1.03% from eq. (6). The uncertainties of axial/radial power distributions were not accounted for in the sensitivity coefficient approach.

The numerical uncertainty of the MATRA code has been assessed using the method of manufactured solution [11]. From a preliminary result of solution uncertainties of the MATRA code for an axial flow, crossflow, and enthalpy, the numerical uncertainty for evaluating DNBR was estimated as 0.76%. As described in Section 2.1, the uncertainty of measured CHF data (u_M) was estimated as 0.68% from the instrumentation error during the CHF experiments. By combining these uncertainties according to eq. (4), the validation uncertainty of the CHF prediction model against this selected CHF data was estimated as 1.45% by the sensitivity coefficient approach.

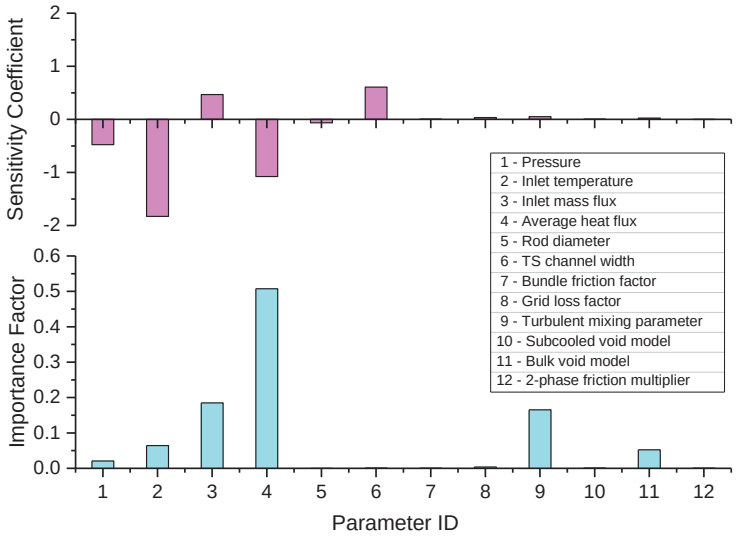

Figure 6. Sensitivity Coefficients and Importance Factors for CHF Lookup Table Method.

3.4. Monte-Carlo Approach

Nonlinear effects on the propagation of input parameter uncertainties to the simulation results were evaluated by employing a direct Monte-Carlo approach. The variation of DNBR was calculated at the minimum DNBR (MDNBR) location for 2000 simple random samplings of each input parameter. Under nominal condition of input parameters, the MDNBR was predicted at the relative axial level of 0.82. A distribution of *E* evaluated from 2000 sets of random input parameters is shown in Fig. 7. The population of *E* was regarded as a normal distribution at a 5% significance level by the Kolmogorov-Smirnov normality test. Because the measured CHF is also applied to predict the CHF through the MATRA code, the measurement uncertainty of the CHF is implied in the uncertainty distribution of DNBR by the Monte-Carlo simulation as well as the input uncertainty.

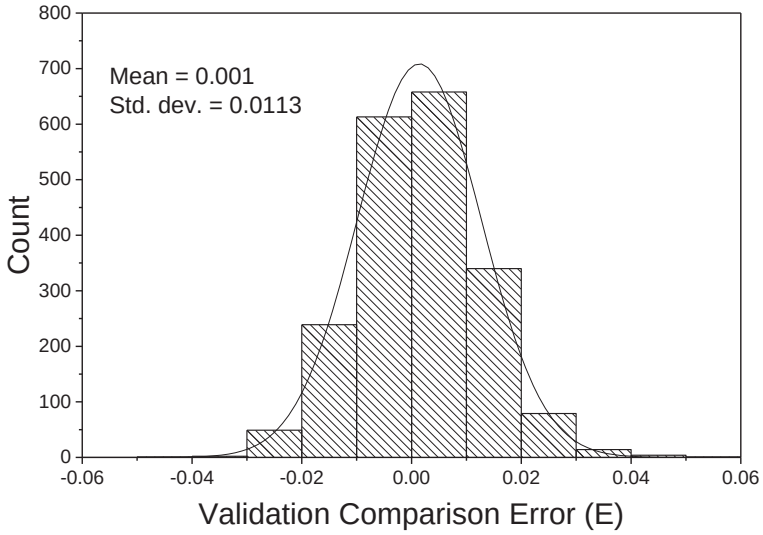

Figure 7. Distribution of DNBR uncertainty by Monte-Carlo approach due to u_{input} and u_M

The combined uncertainty of u_{input} and u_M estimated by the Monte-Carlo approach was compared in Fig. 8 with that estimated by the sensitivity coefficient approach at different axial levels. When the uncertainties of axial and radial power distributions were not considered (Monte-Carlo Approach-1), the combined uncertainty was evaluated as 1.03% while it was 1.23% by the sensitivity coefficient approach. The combined uncertainty increased up to 1.13% when the uncertainties of the power distributions were accounted for (Monte-Carlo Approach-2). By accounting for the numerical uncertainty of the MATRA code, the validation uncertainties of the CHF prediction model by the Monte-Carlo approach with and without the uncertainties of radial/axial power distributions were estimated as 1.36% and 1.28%, respectively.

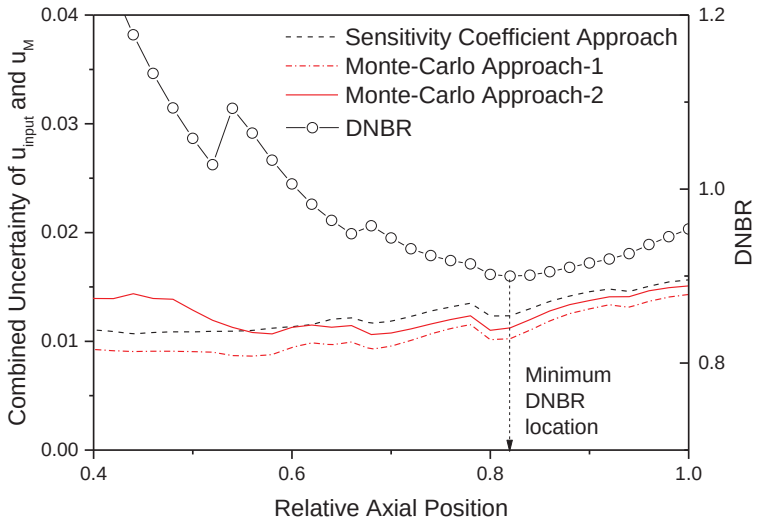

Figure 8. Comparison of uncertainties at different axial level

3.5. Influence of Experimental Uncertainty on the Correlation Limit DNBR

The validation uncertainty evaluated in the preceding sections represents an uncertainty of the normalized P/M (i.e., $\mu_{P/M}$) which accounts for the input uncertainty, measurement uncertainty, and numerical uncertainty. The experimental uncertainty propagates to the predicted CHF through the MATRA code. As a result of the parametric study, it appears that the u_{input} tends to increase as the mass velocity decreases and/or the rod power increases. In this study, the influence of experimental uncertainty on the limit DNBR was illustrated by imposing a single value of validation uncertainty on the CHF database which was employed in section 2.2.

The limit DNBR for a CHF correlation is usually determined from the distribution of M/P which were calculated on the basis of the nominal values of predicted and measured CHF. The correlation limit DNBR can be evaluated by eq. (2) for a normally distributed M/P database. On the other hand, if the experimental uncertainty is accounted for, each M/P becomes a random variable with a standard deviation corresponding to the validation uncertainty. In this case, the correlation limit DNBR for the CHF database can be evaluated by the following procedure:

(i) Conduct a random sampling of P/M for a selected CHF data according to the normally distributed pdf and the validation uncertainty.
(ii) Repeat (i) for all CHF data, and evaluate the correlation limit DNBR ($LDNBR_i$) for the sampled set of database by eq.(2)
(iii) Repeat (i) ~ (ii) for a predetermined number of samples (2000 samples for this study)
(iv) From the mean and standard deviation of the $LDNBR_i$ for the 2000 samples, the correlation limit DNBR considering the experimental uncertainties ($LDNBR_{UNC}$) was evaluated by

$$LDNBR_{\mathrm{UNC}} = \bar{X}_{LDNBR_i} + k_{95/95} \cdot s_{LDNBR_i} \tag{8}$$

where $k_{95/95}$ is 1.703 for 2000 sample data [9]. Figure 9 depicted a relationship between the imposed validation uncertainty and the change of limit DNBR with respect to the reference value (i.e.,

$LDNBR_{ref}$=1.174 as evaluated in section 2.2). When the validation uncertainty of 1.36% estimated from the Monte-Carlo approach was imposed on the 437 CHF data points for the SMART test bundles, it was appeared that the correlation limit DNBR increased about 0.5% by the following equation.

$$\text{Change of Limit DNBR (\%)} = \frac{LDNBR_{UNC} - LDNBR_{ref}}{LDNBR_{ref}} \times 100 \quad (9)$$

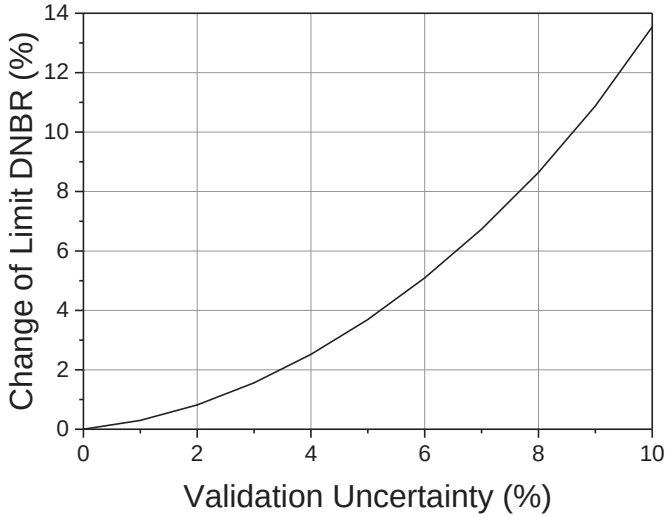

Figure 9. Influence of validation uncertainty to the limit DNBR

4. CONCLUSIONS

An accuracy of the AECL-IPPE 1995 CHF lookup table was evaluated for rod bundle CHF data under advanced PWR conditions. A complementary bundle correction factor, as a function of the pressure, mass flux, and grid spacing, was devised on the basis of local parameters calculated by the MATRA code.

The influence of the CHF experimental uncertainty on the prediction of CHF was examined on the basis of the V&V procedure issued by ASME. From the Monte-Carlo approach with 2000 simple random samplings, the combined uncertainty of u_{input} and u_M was evaluated as 1.13%. By combining with the numerical uncertainty (0.76%), the validation uncertainty of CHF prediction for the selected CHF data was evaluated as 1.36%.

The influence of the validation uncertainty to the limit DNBR was illustrated by imposing a single value of the validation uncertainty on the 437 CHF data points for SMART test bundles. As a result of the analysis, it appeared that the limit DNBR increases about 0.5% when the validation uncertainty of 1.36% was applied to the CHF database.

ACKNOWLEDGMENTS

This work was supported by the National Research Foundation of Korea(NRF) grant funded by the Korea government(MSIP) (No. 2012M2A8A4026261).

REFERENCES

1. D.C. Groeneveld, et. al., "The 1995 Look-up Table for Critical Heat Flux in Tubes," *Nucl. Eng. Des.*, **163**, pp. 1-23 (1996).
2. ASME, "Standard for Verification and Validation in Computational Fluid Dynamics and Heat Transfer," ASME V&V 20-2009, The American Society of Mechanical Engineers (2009).
3. K.K. Kim, et. al., "SMART: The First Licensed Advanced Integral Reactor," *J. Energy Power Eng.*, **8**, pp. 94-102 (2014).
4. D.H. Hwang, S.Q. Zee, M.H. Chang, "A Comprehensive Assessment of Round Tube CHF Prediction Models for Square-Latticed Rod Bundles," *Proceedings of 12th International Heat Transfer Conference (IHTC-12)*, Grenoble, France, August 18-23, pp. 309-314 (2002).
5. D.C. Groeneveld, et. al, "The Effect of Fuel Subchannel Geometry on CHF," *Proceedings of the 5th International Topical Meeting on Reactor Thermal Hydraulics (NURETH-5)*, Salt Lake City, Utah, September 21-24, pp. 683-690 (1992).
6. V.P. Bobkov, "Comparative Analysis of Two Tabular Methods for Calculating Critical Heat Fluxes in Rod Assemblies," *Atomic Energy*, **88**, pp. 268-273 (2000).
7. F. Inasaka and H. Nariai, "Evaluation of Subcooled Critical Heat Flux Correlations for Tubes With and Without Internal Twisted Tapes," *Nucl. Eng. Des.*, **163**, pp.225-239 (1996).
8. L.S. Tong, "Boiling Crisis and Critical Heat Flux," TID-25887, Westinghouse (1972).
9. D.B. Owen, "Factors for One-Sided Tolerance Limits and for Variables Sampling Plans," SCR-607 (1963).
10. D.H. Hwang, et. al., "Uncertainty Analysis for a PSBT Transient DNB Benchmark Exercise Using a Subchannel Code MATRA," *Proceedings of the 15th International Topical Meeting on Reactor Thermal Hydraulics (NURETH-15)*, Pisa, Italy, May 12-17 (2013).
11. H. Kwon, et. al., "Solution Verification of MATRA Code Using MMS," KAERI/TR-5838/2014 (*in Korean*), Korea Atomic Energy Research Institute (2014).